CrossMark

RESEARCH ARTICLE

Chemical characteristics of soluble aerosols over the central Himalayas: insights into spatiotemporal variations and sources

Lekhendra Tripathee[1,2] · Shichang Kang[1,3] (ID) · Dipesh Rupakheti[4] · Zhiyuan Cong[3,4] ·
Qianggong Zhang[3,4] · Jie Huang[4]

Abstract In order to investigate the spatial and temporal variations of aerosols and its soluble chemical compositions of the data gap zone in the central Himalayan region, aerosol samples were collected at four sites. The sampling location were characterized by four different categories, such as urban (Bode), semiurban site in the northern Indo-Gangetic Plain (Lumbini), rural (Dhunche), and semiarid rural (Jomsom). A total of 230 aerosol samples were collected from four representative sites for a yearlong period and analyzed for water-soluble inorganic ions (WSIIs). The annual average aerosol mass concentration followed the sequence as Bode (238.24 ± 162.24 μg/m^3) > Lumbini (161.14 ± 105.95 μg/m^3) > Dhunche (112.40 ± 40.30 μg/m^3) >

Jomsom (78.85 ± 34.28 μg/m^3), suggesting heavier particulate pollution in the urban and semi-urban sites. The total soluble ions contributed to 12.61–28.19% of TSP aerosol mass. The results revealed that SO_4^{2-} and NO_3^- were the major anion and Ca^{2+} and NH_4^+ were the major cation influencing the aerosol composition over the central Himalayas. Calcium played a major role in neutralizing aerosol acidity followed by NH_4^+ at all the sites. The major compound of aerosol was $(NH_4)_2SO_4$ and NH_4HSO_4 in the central Himalayas. Clear seasonality was observed at three observation sites, with higher concentrations during non-monsoon (dry periods) and lower during monsoon (wet period), suggesting washing out of aerosol particles by heavy precipitation during monsoon. In contrast, semiarid sites did not show the clear seasonal trend due to limited precipitation. Stationary sources were predominant over the mobile sources mostly in the remote sites. Principal component analysis confirmed that the major sources of WSIIs in the region were industrial emissions, fossil fuel and biomass burning, and crustal fugitive dusts. Nevertheless, transboundary aerosol transport over the region from polluted cities from south Asia could not be ignored as indicated by the clusters of air mass backward trajectory analysis.

Responsible editor: Gerhard Lammel

✉ Lekhendra Tripathee
  lekhendra.t@gmail.com

✉ Shichang Kang
  shichang.kang@lzb.ac.cn

1   State Key Laboratory of Cryospheric Science, Northwest Institute of Eco-Environment and Resources, Chinese Academy of Sciences, Lanzhou 730000, China

2   Himalayan Environment Research Institute (HERI), Kathmandu, Nepal

3   CAS Center for Excellence in Tibetan Plateau Earth Sciences, Chinese Academy of Sciences, Beijing 100101, China

4   Key Laboratory of Tibetan Environment Changes and Land Surface Processes, Institute of Tibetan Plateau Research, Chinese, Academy of Sciences, Beijing 100101, China

Introduction

Atmospheric aerosols are of major environmental concern as they adversely affect human health (Davidson et al. 2005; Gao et al. 2012), decrease visibility, and alter the climate (Anderson et al. 2002). Rapid urbanization, industrialization, and increasing population are enhancing the concentration of

pollutants in the atmosphere and the ecosystems (Deshmukh et al. 2012; Pandey et al. 2012). Aerosols not only reflect and affect regional characteristics, nevertheless may also affect the global atmospheric environment due to long-distance transport. Therefore, there is an increasing attention to the study of chemical characteristics of atmospheric aerosols and it is crucial. Moreover, data on chemical composition of aerosols from different environments can form a valuable reference for understanding the evolution of the atmosphere with respect to the speedy development in the industries, energy, and transportation.

Water-soluble inorganic components consist of a large portion of aerosol particles and, hence, play an important role in understanding the chemical reactions in ambient atmosphere (Kumar and Yadav 2016). The water-soluble ions in aerosols can provide valuable information for understanding their physical and chemical characteristics, sources, behavior, and formation mechanism (Wang et al. 2005). Furthermore, it also provides knowledge on the effect of regional and local pollution and the ecosystem health (Tripathee et al. 2016b; Wang et al. 2005). Moreover, spatial and temporal variations of ionic components can be very significant as several aspects such as climatic and orographic features, emission rates of gaseous precursors, and long-range transport of pollutants control them.

Himalayas is regarded as a crucial and very sensitive area regarding the dynamics of atmospheric circulation with its role in meteorology and climate at a regional to global scale (Kang et al. 2010). Atmospheric aerosols build up during dry period in the southern side of the Himalayas and are lifted by Himalayan topography to a higher altitude (Zhao et al. 2013). Furthermore, "brown cloud" attains a vertical thickness of about 3 km, can extend from the Indian Ocean to the Himalayan range mostly during the dry season (Ramanathan et al. 2005), and affect Himalayan population and the environment. Given the importance of atmospheric aerosols on the environmental health and the climate system, several studies have been conducted on aerosol ionic chemistry over the northern side of the Himalayas in the Tibetan Plateau (Cao et al. 2009; Cong et al. 2015; Ming et al. 2007; Zhang et al. 2012, 2010; Zhao et al. 2013) and over the Indian plains and western Himalayas (Deshmukh et al. 2011; Kumar and Sarin 2010; Kumar and Yadav 2016; Ram et al. 2012; Rastogi and Sarin 2005; Safai et al. 2010), during the last decade. Those studies have reported lower soluble aerosols loadings in the northern side of the Himalayas. Therefore, TP could be regarded as an ideal location to monitor the background atmospheric chemistry (Cong et al. 2007). Meanwhile, the Indian plains were reported to have higher aerosol chemical loadings which could have transboundary environmental effects over the Himalayas due to long-range transport. Such long-term

studies on chemical characterization and source identification of aerosols with spatial variations are still limited in the Himalayan regions of Nepal (Carrico et al. 2003; Decesari et al. 2010; Shrestha et al. 1997, 2002; Tripathee et al. 2016b). Therefore, the composition and concentration of pollutants may vary greatly from region to region in the atmosphere. Thus, there is a need to advance knowledge on how inorganic ions formations from different environment vary and differ from one another in the region.

Air pollution has become a serious problem in South Asia, especially in the Himalayan regions of Nepal. The southern side of the Himalayan region is facing long-term poor air quality problems with aerosol as a major pollutant. The atmospheric environment is affected by the transport of short- and long-range pollutants from highly urbanized locations (Tripathee et al. 2014a, b). Investigation of aerosol chemistry in the Himalayan region in Nepal has been limited on a temporal and spatial scale to date, mainly due to its remoteness and difficult topography. Therefore, special attention is needed for systematic long-term study of aerosols in the region from urban, semi-urban to the remote sites to fulfill the research gaps in the region.

In this paper, we present the results from 1-year measurements of the water-soluble inorganic ions of aerosol collected at four sites including different representative environments in the central Himalayas, Nepal. The main aim is to provide the comprehensive insights on chemical compositions, seasonal and spatial variations of aerosols, and soluble ionic species profiles with different environmental gradients. Nevertheless, this study also tries to investigate the acidification/neutralization potential of aerosols and evaluate the possible sources of these inorganic soluble aerosols over the central Himalayan region.

Experimental methods

Sampling site description

Four sites were chosen to investigate the characteristics of aerosols using total suspended particles (TSP) since early spring of 2013. The details on sampling sites are presented in Fig. 1 (Table S1). Sampling was carried out from two transects from south-to-north which includes four sites along the Himalayas. The locations of the sites are characterized by four different categories, such as urban (Bode), semi-urban (Lumbini), rural (Dhunche), and semiarid rural (Jomsom) (Fig. 1) and location pictures are presented in Fig. S1. The more detailed information about the sites is described as the following:

1. Bode is situated in the Bhaktapur district of Nepal in the Kathmandu valley and is located at 85.38° E and 27.67° N. Kathmandu valley is the largest urban city in Nepal

Fig. 1 Location of sampling sites over the central Himalayas
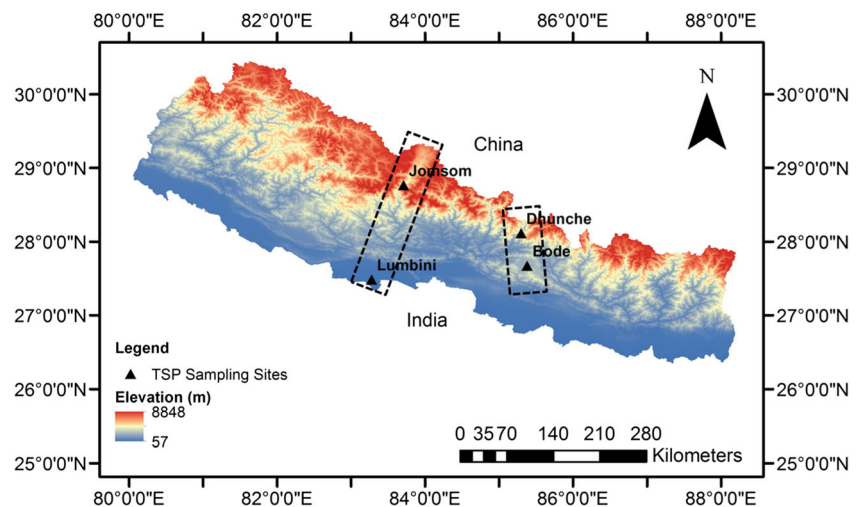
with a population of about 1 million. Overall, the characteristics of the site consist of lots of regional polluting sources. It is surrounded by a large number of anthropogenic emission sources such as factories, waste burning, and vehicular emission. Numerous brick kilns are located within the vicinity of the site. The TSP sampler was placed at the roof of the residential house that is about 10 m above the ground.

2. Dhunche is a small town located between the Ganesh and the Langtang sub-range of the central Himalayas located at 85.30° and 28.11°. The air masses at this site are defined by the mountain–valley wind system. Afternoon hours are dominated by southerly winds, which can transport considerable amounts of aerosols from the upwind areas reaching as far as the IGP. Extensive biomass burning is performed in the fields covering the valley slopes in this region. Moreover, local household activities (mainly combustion of biomass) may play an important role in determining the peak hours of aerosol emissions pollution source around the valley.

3. Lumbini is located in the Rupandehi district of southern lowland of Nepal at the elevation of ~ 100 m a.s.l. Being archeologically a rich place (birth place of Lord Buddha), Lumbini was declared as World Heritage site by UNESCO in 1997. So, the area observes the movement of tourists from around the world. Lumbini lies in the northern Indo-Gangetic Plain (IGP), which is one of the most populous and polluted regions of the world comprising parts of Pakistan, India, Nepal, and Bangladesh. The majority of the population in IGP use biomass as cooking fuel. Other sources of emission in the IGP are coal-based thermal power plants, industries, transportation, brick kilns, mining, and crop residue burning. The TSP sampler was placed on the rooftop of water tower about the height of 5 m (83.28° E and 27.48° N).

4. Jomsom is a small and dry town located in the rain shadow zone of half hills in the central Himalayas. This site experiences the lowest precipitation (less than 300 mm per annum) and also regarded as a semiarid region (Sigdel and Ma 2016). The major human activities are tourism and limited agricultural activities. Since it is a rural site with minimal local emissions, the site can represent a regional background location in Nepal. The TSP sampler was placed on the roof of the laboratory on about 2 m above the ground surrounded by high mountains (83.71° E and 28.76° N).

In general, the climate of this region is controlled by the Indian summer monsoon system during summer (mid-June–September), which is characterized by relatively high temperature and humid weather with prevailing southerly winds. In the other remaining period, westerlies dominate the large-scale atmospheric circulation pattern, which brings limited precipitation in the whole region that covers all four sampling sites (Tripathee et al. 2014b).

Aerosol collection and laboratory analysis

For a yearlong period (April 2013 to March 2014), aerosol samples were collected weekly at four sites in the southern side of the central Himalayas (Fig. 1). Medium-volume samplers (KC-120H, Laoshan Co., 5 flow rate: 100 L min^{-1} at standard condition) were used for the aerosol sampling. The sampling duration of each sample was 24 h. Aerosol samples were collected using 90-mm-diameter quartz filters (QM/A, What-man, UK), which were pre-baked at 450 °C for 6 h in order to eliminate residual impurities. To avoid the contamination, extreme care was taken during sample collection and handling. Gloves and mask were worn all time during the sampling. After the sampling, the filters were

kept in the disc and then wrapped with aluminum foil. All the collected samples were kept in the refrigerator at 4 °C before the laboratory analysis.

An aliquot of the filter (1.6 cm^2) was extracted with 10-mL ultrapure water (18.2 MΩ/cm resistivity). Then, the water-soluble ionic components (Cl$^-$, SO$_4^{2-}$, NO$_3^-$, Ca^{2+}, Na$^+$, K$^+$, Mg^{2+}, and NH$_4^+$) were analyzed using an ion chromatograph at the State Key Laboratory of Cryospheric Science, Chinese Academy of Sciences. Anions were analyzed using ICS-1500 and cations were determined by Dionex-320. In brief, both the systems consisted of a separation column (CS12A (4 × 250 mm) for cations and ASII-HC (4 × 250 mm) for anions). Further, it contained of a guard column (CG12A for cations and AGII-HC (4 × 50 mm) for anions) and a self-regenerating suppressed conductivity detector (CSRS UltraII-4 mm for cations and ASRS300–4 mm for anions). Cations were eluted with 20 mM methanesulfonic acid (MSA) and anions were eluted using a 11-mM sodium hydroxide (NaOH) solution. The recovery of each ion was found to be in the range of 80–118%. In addition, the quality assurance was regularly done by using Standard Reference Materials (GBW08606), produced by National Research Center for Certified Reference Materials, China. The details on laboratory analysis have been explained elsewhere (Tripathee et al. 2016b; Xu et al. 2014). The detection limit for cations and anions was 0.01 μg m^{-3}, which was calculated using the air volume of actual samples. The relative standard deviation (RSD) percent for each ion were less than 5%. Field blank filters were subjected to the similar extraction and preparation procedures as for the actual particulate sample filters and was measured by exposing the filters in the sampler without drawing air. Mostly, they denoted less than 5% of a measured sample concentration.

TSP mass loadings were determined gravimetrically. The collected filter weight was measured twice before and after sampling and the net accumulation mass for each filter was calculated as the difference between the pre and post sampling weight microbalance, after equilibration at constant temperature and humidity (20 °C, 39%) for 24 h.

Results and discussion

Overview of annual aerosol mass and water-soluble inorganic ions (WSIIs) in TSP

The annual average TSP mass and water-soluble inorganic ions (WSII) concentrations from four sampling sites for a 1-year period is summarized in Table 1. The annual average TSP mass concentration was observed to be highest at the urban site Bode (238.24 ± 162.24 μg/m^3) followed by semi-urban site in northern Indo-Gangetic Plain (IGP) Lumbini (161.14 ± 105.95 μg/m^3), rural site Dhunche

(112.40 ± 40.30 μg/m^3), and semiarid rural site Jomsom (78.85 ± 34.28 μg/m^3). The aerosol loadings in two sites Bode and Lumbini were comparable with the urban sites in the northern India (Kumar and Yadav 2016; Ram et al. 2012), and significantly lower at rural sites Jomsom and Dhunche, suggesting heavier aerosol load in the urban and semi-urban sites than on remote sites in the central Himalayas. The emissions from brick kilns could not be ignored for urban sites in Nepal, as they contribute to higher loadings TSP aerosols mostly in dry operational periods. The total WSIIs accounted for 21.01, 28.19, 19.15, and 12.61% of the total TSP load at our sites similar to the observations in the Indian plains (Deshmukh et al. 2012; Kumar and Yadav 2016; Ram et al. 2012).

The mass percentage loadings of eight WSIIs are shown in Fig. S2. From anions, SO$_4^{2-}$ was the dominant component at all the sampling sites followed by NO$_3^-$ and Cl$^-$. Overall, SO$_4^{2-}$ and NO$_3^-$ together accounted for highest anion mass percentage 34.72, 31.04, 41.41, and 43.53% in Lumbini, Jomsom, Bode, and Dhunche, respectively, that is attributed to secondary formation from their precursor gases (Fig. S2). In details, the major sources for the anions SO$_4^{2-}$ and NO$_3^-$ in the atmosphere are from the oxidation of their gaseous precursors, SO$_2$ and NO$_x$, which are emitted from different anthropogenic activities (Safai et al. 2010). In the urban sites, these precursor gases (SO2 and NOx) are emitted significantly from brick kilns. The NO$_3^-$ concentrations are found to be lower than SO$_4^{2-}$ in the central Himalayas. However, in the case of cations, Ca^{2+} was the dominant component followed by NH$_4^+$ and Na$^+$ at two urban sites Bode and Lumbini, and Ca^{2+} followed by Na$^+$ and NH$_4^+$ in semiarid site Jomsom. Meanwhile, at the remote site Dhunche, Na$^+$ had the highest percentage followed by Ca^{2+} and NH$_4^+$. Higher mass percentage of crustal ion Ca^{2+} and anthropogenic NH$_4^+$ was also reported in the central Himalayan regions of Nepal by wet atmospheric deposition (Tripathee et al. 2014b). Moreover, the comparison among different observed sites indicates that crustal ions had a more significant influence in the semi-urban site and especially on semiarid region whereas in the urban sites, anthropogenic influence seemed to be dominant. Meanwhile, the total mass concentrations percentage of the analyzed ionic species of secondary ions (SO$_4^{2-}$, NO$_3^-$) and NH$_4^+$ occupied about 47.75, 34.45, 56.86, and 58.44% at Lumbini, Jomsom, Bode, and Dhunche, respectively, suggesting that the three investigated sites during the sampling period were under strong anthropogenic influence from regional and long-range transport. Further, the mass percentage of (Ca^{2+} and Mg^{2+}) accounted for 28.56, 43.82, 22.42, and 15.74% in Lumbini, Jomsom, Bode, and Dhunche indicating that the semiarid region (Jomsom) is mainly influenced by local crustal source (carbonate rich dust) rather than the major anthropogenic sources.

Table 1 Summary of annual average concentrations of aerosol mass and water-soluble inorganic ions (WSII) in comparison with neighboring regions

	This study				Nearby regions						
					Himalayas		Mt. Yulong, TP	Agra India	Delhi India	Durg City, India	Manora Peak
					Southern	Northern					
Variables	Lumbini ($n = 50$)	Jomsom ($n = 46$)	Bode ($n = 73$)	Dhunche ($n = 61$)	a	b	c	d	e	f	g
TSP mass	161.14 ± 105.95	78.85 ± 34.28	238.24 ± 162.24	112.40 ± 40.30							
Cl^-	0.79 ± 0.89	0.27 ± 0.34	2.17 ± 2.25	0.34 ± 0.60	0.06	0.02	0.26	4.6	8.23	3.23	–
NO_3^-	3.63 ± 3.55	1.64 ± 1.53	5.38 ± 4.72	1.95 ± 1.72	0.78	0.20	0.57	6.7	15.13	5.63	1.10
SO_4^{2-}	6.38 ± 4.21	3.79 ± 2.89	10.96 ± 10.08	4.06 ± 2.73	1.41	0.43	1.77	5.9	16.74	8.88	6.40
Na^+	3.00 ± 1.81	2.59 ± 1.23	3.36 ± 1.65	2.30 ± 1.66	0.12	0.07	0.22	4.0	5.76	1.75	–
NH_4^+	3.78 ± 3.52	0.96 ± 1.03	6.17 ± 6.57	2.17 ± 2.03	0.54	0.03	0.37	2.7	6.06	5.18	–
K^+	3.01 ± 2.44	0.58 ± 0.72	2.62 ± 3.39	0.94 ± 1.15	0.20	0.02	0.26	3.5	4.11	0.87	0.70
Mg^{2+}	0.60 ± 0.55	0.31 ± 0.18	0.65 ± 0.68	0.19 ± 0.13	0.05	0.88	0.08	1.4	1.30	0.80	0.30
Ca^{2+}	7.60 ± 6.70	7.35 ± 4.78	8.19 ± 7.46	2.17 ± 1.47	0.66	0.04	3.93	6.7	6.82	2.53	1.80
WSII	28.96 ± 18.72	17.48 ± 9.75	39.22 ± 32.98	14.13 ± 8.83							
%WSII	21.01	28.19	19.15	12.61							
	TSP annual	TSP annual	TSP annual	TSP annual	PM10 dry period	TSP annual	TSP winter	TSP annual	PM10 annual	PM10 annual	TSP 42 months

a–Carrico et al. 2003, b–Cong et al. 2015, c–Zhang et al. 2012, d–Satsangi et al. 2013, e–Chelani et al. 2010, f–Deshmukh et al. 2012, g–Ram et al. 2010

Water-soluble inorganic ions (WSIIs) from central Himalayas with comparison to nearby regions

The average annual concentrations of major WSIIs from this study are compared with the literature reported from nearby locations of the Tibetan Plateau and India and are presented in Table 1. In this study, majority of ions in aerosols accounted for Ca^{2+} and SO_4^{2-}, which is similar to the findings from Agra, India. The results from Lumbini (semi-urban site in IGP close to the Indian border), possess the similar atmospheric environment as in Indian cities (Deshmukh et al. 2012; Satsangi et al. 2013), suggesting that the site may have been affected from the aerosols transported from southern Indo-Gangetic Plains (IGP). In comparison with the Tibetan Plateau, higher concentrations of WSIIs in aerosols over urban location suggest the heavier pollution in the urban and IGP region of Nepal. Furthermore, dust aerosol Ca^{2+} concentrations in southern Himalayan region were found to be higher as compared to the TP (Zhang et al. 2012) and the higher Himalayas (Carrico et al. 2003; Cong et al. 2015). Such results are not surprising as the southern slope of Himalayas is experiencing higher loadings of dust aerosols in the environment from the construction activities and regional sources. Previous studies from precipitation chemistry have also suggested the high concentration of crustal components in the southern Himalayan regions (Tripathee et al. 2014a, b). In

addition, anthropogenic soluble ions (e.g., SO_4^{2-}, NO_3^-, and NH_4^+) in this study from high-altitude sites are found to be significantly lower than the urban sites in India, and were comparable to the Manora Peak, high-altitude site in western India (Ram et al. 2010). The concentrations of major soluble ions at remote sites Dhunce and Jomsom were similar to the concentrations in Monora Peak suggesting that these sites could be considered as background sites; however, Ca^{2+} in Jomsom was higher due to higher dust loadings in semiarid site. However, in the urban sites Bode and Lumbini, such ions are found to be in similar concentrations labels as in the Indian plains (Chelani et al. 2010; Deshmukh et al. 2012; Satsangi et al. 2013), suggesting that the urban atmospheric environment in Nepal is comparable to the Indian plains. However, the rural sites from Nepal have lower concentrations as compared to the Indian sites and are slightly comparable to remote sites in the Tibetan Plateau, suggesting that these sites can be regarded as background sites for atmospheric chemistry studies.

Ionic balance and acid neutralization

Charge balance

Ion balance calculations are important for estimating the acid–base balance of the aerosol particles in the atmosphere and are

good indicator to understand acidity of aerosol. Therefore, micro equivalents of cation and anion in TSP aerosol samples were calculated as (Shen et al. 2009):

CE (*Cation Equivalent*)

$$= Na^+\big/23 + NH_4^+\big/18 + K^+\big/39$$
$$+ Mg^{2+}\big/12 + Ca^{2+}\big/20 \qquad (1)$$

AE (*Anion Equivalent*)

$$= SO_4^{2-}\big/48 + NO_3^-\big/62$$
$$+ Cl^-\big/35.5 \qquad (2)$$

The relationship between anion and cation equivalents for all the samples at different seasons are shown in Fig. 2. A good correlation was observed between anion and cation equivalents at all four sites. Meanwhile, lowest correlation was observed during post-monsoon ($r = 0.36$, $p < 0.01$) in Jomsom and during monsoon ($r = 0.55$, $p < 0.01$) in Bode. However, except those, strong correlation ($r > 0.65$ to $r = 0.94$, $p < 0.01$) were observed at all the sites in all seasons. Such a result is an indication that these major soluble ions existed in submicron particles in the central Himalayas (Shen et al. 2009). Moreover, it can be noted from the Fig. 2 the slope of the regression line is lower than unity at all sites and during all seasons, implying that the aerosol samples tend to be of alkaline nature in the region. Further, the average CE/AE equivalent ratio was also calculated for all sites to further understand the aerosol characteristics. The CE/AE equivalent ratios for Lumbini, Jomsom, Bode, and Dhunche were found to be 3.78, 4.49, 5.26, 2.30, and 2.93, respectively, which is larger than unity, that also confirms the cationic domination on the anionic composition suggesting the alkaline nature of aerosol (Sun et al. 2006; Yang et al. 2016). Various previous studies have also suggested that the anion deficiency is mainly due to exclusion of HCO_3^-/CO_3^{2-} detection (Al-Khashman 2005; Zhang et al. 2012) and organic acids; however, concentrations of organic acid are very low in our region (Tripathee et al. 2014b). In addition, if it failed to detect the anion (HCO_3^-/CO_3^{2-}), the relationship between Ca^{2+} and ΔC (CE-AE) should have significant positive correlations (Sun et al. 1998; Zhang et al. 2012). The correlation between Ca^{2+} and ΔC (CE-AE) at our sampling sites were found to be very strong ($R^2 > 0.79$; $p < 0.01$) (Fig. S3), implying that HCO_3^-/CO_3^{2-} should be the major unmeasured anion at our sites. Therefore, the dominant inorganic compound at our sampling sites must be $CaCO_3$. Our results are consistence with the prior studies in the Lijiang city (Zhang et al. 2011) and Mt. Yulong, southeastern Tibetan Plateau (Zhang et al. 2012).

Furthermore, attention has been given to SO_4^{2-} and NH_4^+ and their ratios as they are the important component of the tropospheric aerosol (Ram et al. 2012; Zhang et al. 2012). As pointed out by Zhang et al. (2012), if the equivalent ratio of NH_4^+/SO_4^{2-} is 0.5–1, it suggests that ammonium and sulfate exists mainly as $(NH_4)_2SO_4$ and NH_4HSO_4, and if the equivalent ratio is >1, it suggests near-complete neutralization of sulfuric acid and their existence as $(NH_4)_2SO_4$ and NH_4NO_3. In this study, the mean equivalent ratio of NH_4^+/SO_4^{2-} at three sites Lumbini, Bode, and Dhunche were (1.41 ± 0.83), (1.41 ± 0.62), and (1.23 ± 0.70), respectively, suggesting that in these three sites, ammonium exists as $(NH_4)_2SO_4$. Such a result was also observed in the urban sites in the Indo-Gangetic Plain in India (Ram et al. 2012) and aerosol sampled at Lijiang City (Zhang et al. 2011). Moreover, a good correlation coefficient was observed between NH_4^+ and nss-SO_4^{2-} ($R^2 > 0.62$, $p < 0.01$) at these three sites which also supports our finding (Fig. S4). However, in the semiarid remote site, the ratio was (0.64 ± 0.51), indicating the main compound composed of NH_4^+ and SO_4^{2-} in Jomsom is NH_4HSO_4. Prior study on aerosol in the Hidden Valley on the southern side of the Himalayas also showed the similar equivalent ratio 0.69 (Shrestha et al. 1997), which lies in the similar location as Jomsom in the western Himalayas, Nepal.

Neutralization of aerosol acidity

Acid neutralization capacity of different cations can be estimated by calculating the neutralization factors (NF). The calculation is based on the fact that, in aerosols, the major acidifying anions are SO_4^{2-} and NO_3^- and the major acid neutralizing cations are Ca^{2+}, NH_4^+ and Mg^{2+}. It has been assumed in many studies that Cl^- and Na^+ originate solely from sea in the form of sea salt and hence Na^+ and Cl^- were neglected in the prior studies for the calculation of NF (Safai et al. 2010; Satsangi et al. 2013). However, at our sites, poor correlation of Na^+ and Cl^- was observed at all sites, $r = 0.14$, 0.37, 0.34, and 0.52 at Lumbini, Jomsom, Bode, and Dhunche, respectively, and lower ratio Cl^-/Na^+ (< 1.16) was observed at all sites, indicating possible different origin of Cl^- (Xu et al. 2017). Meanwhile, complex chemical processes occurring in the soil to convert some amounts of Na^+ and Cl^- into some other forms may be the reason for their poor correlations. In addition, Himalayas with their sedimentary origin would have significant amount of NaCl buried in soil, which may have exposed in the atmosphere with construction activities causing difference from sea salt composition; however, it may have less contribution. In our samples, the concentrations of Na^+ was observed to be higher than Cl^-, suggesting that there must have been loss process of Cl^- on sea salt particles, which clearly explains the lower ratios of Cl^-/Na^+ in all observations sites over the central Himalayas (Wu et al. 2006). The details on loss process of Cl^- in aerosol particles have been described elsewhere (Wu et al. 2006). Therefore, the role of Cl^- in
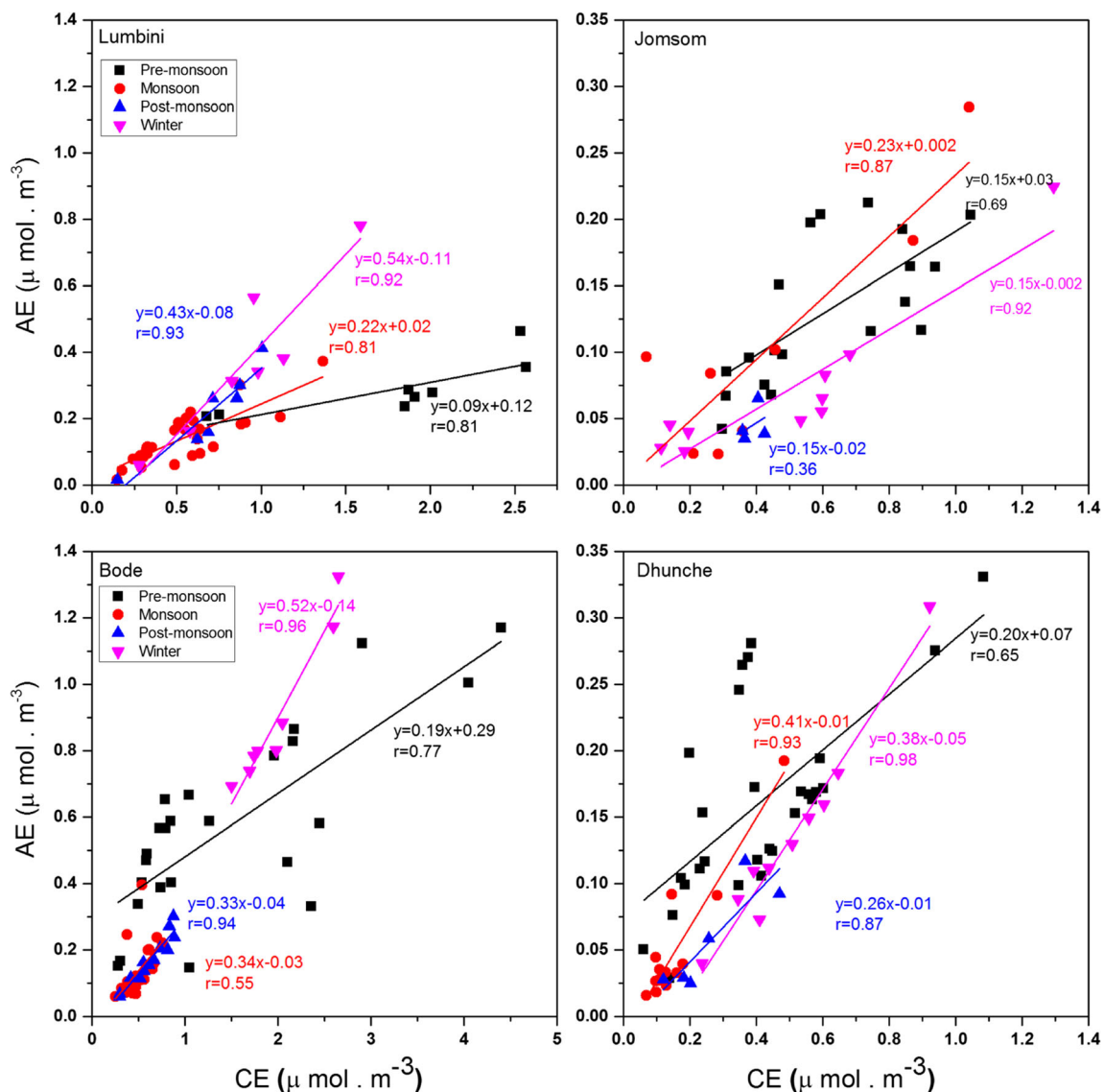
Fig. 2 Plot showing anion equivalents (AE) versus cation equivalents (CE) in different seasons

neutralization process could not be neglected in this study. As assuming that the Na^+ was derived from ocean only and mostly existed as NaCl in sea salts (Satsangi et al. 2013), so sea salt [Cl^-] can be obtainable as [Na^+]/1.1 based on their sea water ratio. Moreover, non-sea salt [Cl^-] can be calculated by deducting [Na^+]/1.1 from [Cl^-] (Xu et al. 2017), and the NFs were calculated from the following equations:

$$NF\left(nss-Ca^{2+}\right)$$
$$= [nss-Ca^{2+}]/([nss-SO_4^{2-}] + 2[NO_3^-] + 2[Cl^-]-2(Na^+/1.1)) \quad (3)$$

$$NF\left(nss-Mg^{2+}\right)$$
$$= [nss-Mg^{2+}]/([SO_4^{2-}] + 2[NO_3^-] + 2[Cl^-]-2([Na+]/1.1)) \quad (4)$$

$$NF\left(NH_4^+\right)$$
$$= [NH_4^+]/2[nss-SO_4^{2-}] + [NO_3^-] + [Cl^-]-([Na]/1.1)) \quad (5)$$

The calculated annual average NF values from four sites are presented in Table 2. As expected, the largest acid neutralizing agent in the central Himalayas are nss-Ca^{2+} followed by NH_4^+ and Mg^{2+}. However, in the semiarid site Jomsom, Ca^{2+} is the only major acid neutralizing agent (NF = 3.14) and nss-Mg^{2+} (0.26) and NH_4^+ (0.28) showed insignificant role which must be because of higher loadings of calcium rich dust in the dry atmosphere. Nevertheless, it can be noted from this study that nss-Mg^{2+} plays a negligible role on acid neutralizing over the central Himalayas which is also supported by the previous findings of NFs in precipitation chemistry (Tripathee et al. 2014b) and aerosol in the southern Himalayan valley (Tripathee et al. 2016b). Nevertheless, previous study has

Table 2 Neutralization factor for soluble ions in TSP collected over Central Himalayas

Sites	NF (Ca^{2+})	NF (NH_4^+)	NF (Mg^{2+})
Lumbini	1.72 ± 0.97	0.58 ± 0.31	0.21 ± 0.13
Jomsom	3.14 ± 1.86	0.28 ± 0.22	0.26 ± 0.19
Bode	1.33 ± 0.74	0.57 ± 0.24	0.16 ± 0.07
Dhunche	0.86 ± 0.37	0.52 ± 0.30	0.12 ± 0.04

suggested that source and fate of N-compounds emitted from natural or anthropogenic sources are very difficult to establish (Pathak et al. 2009) and ammonia could be the major neutralizing agent when the atmospheric concentrations of NH_4^+ are higher. However, TSP aerosols at our sites were Ca^{2+} rich than ammonium which may have resulted in calcium as the largest neutralizing agent over the studied region.

Furthermore, in order to understand the complete neutralization of HNO_3 and H_2SO_4 by NH_4^+, the equivalent ratios of $NH_4^+/(NO_3^- + SO_4^{2-})$ were also calculated. The ratio value of unity would indicate the complete neutralization of acidity by NH_4^+ (Kumar and Yadav 2016). The average equivalent ratio in TSP from the sampled sites were 0.81 ± 0.47, 0.49 ± 0.40, 0.79 ± 0.40, and 0.83 ± 0.52 in Lumbini, Jomsom, Bode, and Dhunche, respectively. Such a result is an indication that there could be cations other than NH_4^+ which may play a role in neutralizing acidic species in the central Himalayan region. Moreover, the oxidation of the gaseous precursors (SO_2 and NO_x) in the atmosphere produces SO_4^{2-} and NO_3^- ions that are mainly neutralized by crustal aerosols (e.g., Ca^{2+} and Mg^{2+}) and ammonia (Satsangi et al. 2013). The correlation coefficient between the sum of (NO_3^- + nss-SO_4^{2-}) and (nss-Ca^{2+} + NH_4^+) is presented in Fig. 3. The good correlation coefficient was observed between their sums with ($r = 0.77$, 0.58, 0.88, and 0.84 at Lumbini, Jomsom, Bode, and Dhunche, respectively), further confirms that Ca^{2+} and NH_4^+ play a major role in neutralizing the acidity in the aerosols of southern Himalayas.

Spatial and temporal variation of WSIIs over the central Himalayas

Spatial variation of soluble ions

The total annual average concentration of TWSIIs at four sites is presented in Table 1 (Fig. S5). The annual concentrations from the central Himalayas followed the order as follows: B o d e (39.22 ± 32.98 μg m^{-3})> L u m b i n i (28.96 ± 18.72 μg m^{-3})> Jomsom (17.48 ± 9.75 μg m^{-3}) >Dhunche (14.13 ± 8.83 μg m^{-3}), which contributed to 12.61–28.19% of aerosol mass (Table 1). Overall, among the investigated ions at first transect (Jomsom and Lumbini), followed the order of Ca^{2+}> SO_4^{2-}> NO_3^-> NH_4^+, meanwhile

at second transect (Bode and Dhunche) followed SO_4^{2-}> Ca^{2+}> NH_4^+> NO_3^-, indicating complex and heterogeneous aerosols in the region. Such results also suggest that the central Himalayan region is influenced by mixed regional and local aerosols, which must have derived from fugitive dust (soil) and anthropogenic influences of aerosol particles (Wu et al. 2006). Further, higher loadings of major soluble ions observed in urban and semi-urban sites suggest that fossil fuel plays a major role in those sites. Moreover, SO_4^{2-}, NO_3^-, and NH_4^+ rich aerosols are formed through gas to particle conversion processes. In this process, the respective precursor gases for these aerosol (SO_4^{2-} and NO_3^-) get oxidized when it reacts with H_2O in the atmosphere and then NH_4 is formed from reduction of its precursor NH_3 (Safai et al. 2010). Such precursor gases are emitted from various anthropogenic sources such as industrial, fossil fuel, and domestic activities.

Temporal variation of soluble ions in the central Himalayas

The temporal variations of major soluble ionic components in the aerosol collected at four sites in the central Himalayas, Nepal is shown in Fig. 4, and concentration at four seasons is shown in Table 3. A clear evidence of seasonality was observed for the major WSIIs at three sites (Lumbini, Bode, and Dhunche). It was interesting that there was no distinct seasonal variation observed in semiarid background site at Jomsom, which is an indication of very low precipitation compared to other sites (Table S1). Prior study has suggested that low precipitation enhances anthropogenic and natural dust resuspension and limits the deposition of atmospheric particles by wet deposition (Nicolás et al. 2008). In most of the sampling sites, the concentrations of major soluble anthropogenic secondary ions (SO_4^{2-}, NO_3^-, and NH_4^+) were higher during winter, pre-monsoon, and post-monsoon season (dry periods). As explained earlier, nearby Bode and Lumbini sites, there are number of brick kilns that operate during the non-monsoon seasons (November–May). In urban and semi-urban sites, there exist high concentrations of SO_x and NO_x in ambient air, during brick Kilns operational period mainly during dry periods. Therefore, the high concentrations of SO_4^{2-} and NO_3^- ions during dry periods in those sites must have been enhanced by low-grade coal burning (containing high sulfur and high ash) from the kilns. Prior studies have suggested that regional pollution sources in northern India are predominant during winter months (Kumar and Sarin 2010; Satsangi et al. 2013). Higher concentrations during winter may be attributed to the enhanced emissions from heating sources, increased anthropogenic activities, such as vehicular traffic, fossil fuel burning, industrial activities, and inactive atmospheric conditions (low temperature, low wind speed, low mixing height) (Deshmukh et al. 2012; Satsangi et al. 2013). Furthermore, the shift from the gas phase of nitric acid to particle phase of nitrate is favored in low temperature, which might lead to high concentration of

**Fig. 3** Regression between NH_4^+ and nss-Ca^{2+} with NO_3^- and nss-SO_4^{2-}
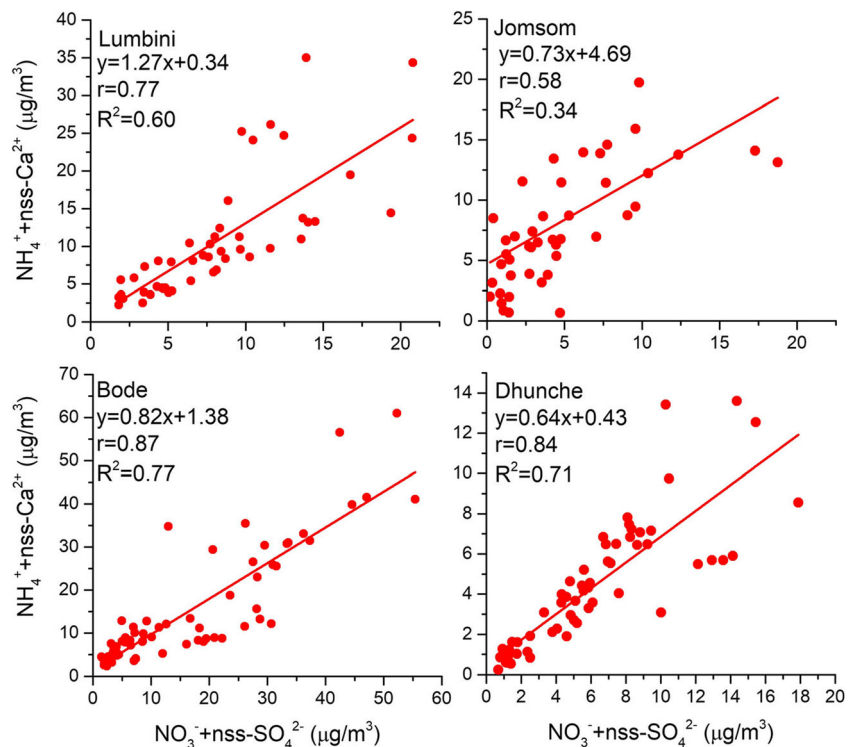
NO$_3^-$ during the winter season. Moreover, a study by Mouli et al. (2006) suggested that a lower concentration of NO_3^- during summer can be due to the volatilization of NH_4NO_3, which increases in higher temperature. In addition, the higher concentrations were also observed during pre-monsoon at rural sites Dhunche and Jomsom, which must be due to the air masses brought by westerlies with little precipitation and more aerosols in the atmosphere during the pre-monsoon season.

In addition, the combination of distinctive weather conditions occurs in this region, i.e., long dry period (non-monsoon season) extending from October to May and the unique geophysical features enhances the accumulation of atmospheric pollution during this period. This gives rise to the regional scale plumes of air pollutants, known as atmospheric brown cloud (ABC). These ABC haze has been observed over the southern side of the Himalayas during winter and pre-monsoon dry periods (Bonasoni et al. 2010; Chen et al. 2017; Lelieveld et al. 2001; Ramanathan and Ramana 2005). Therefore, such pollutants concentrated over the Himalayan atmosphere could enhance the higher loadings of anthropogenic soluble ions during this period (Tripathee et al. 2014b, 2016b), as ABC is composed of major ions such as SO_4^{2-}, NO_3^-, K^+, NH_4^+, dust particles, and also organic components such as black carbon (Ramanathan and Ramana 2005). Heavy atmospheric pollution and less scavenging during the non-monsoon season could cause higher concentrations of these ions in the central Himalayan region with poor air quality, which may have significant impact on human health and the ecosystem in the region.

Calcium (Ca^{2+}) and magnesium (Mg^{2+}) are the typical tracer of crustal source (Ali et al. 2012); and the dry season is favorable for the resuspension of soil particles. A significant correlation coefficient was observed between Ca^{2+} and Mg^{2+} ($R^2 > 0.85$, $p < 0.01$) at all four sites indicating their common sources in Fig. S5. At the same time, desert dust could be transported by westerlies, which are likely regionally long-range transported to the Nepal Himalayas (Carrico et al. 2003), which may play important role in increasing crustal aerosols during the dry period. In addition, prior study in the western Himalaya, India have suggested increase in the concentration of mineral dust related with the long-range transport from desert regions during pre-monsoon period (Ram et al. 2010), which may also contribute to the dust aerosols during the dry periods. Nevertheless, higher concentration of Ca^{2+} during the pre-monsoon could also most reasonably attribute to the high concentrations of fugitive dust during dry period and low precipitation (Chelani et al. 2010). However, in semi-arid site, there was no significant trend in Ca^{2+} concentrations at different seasons throughout the year indicating local sources were dominant and low precipitation enhanced limited deposition of particles from the atmosphere.

K^+ is a biomass burning tracer (Chelani et al. 2010; Deshmukh et al. 2012), and the major fuel used for cooking and heating activities in this region is biomass (Ram and Sarin 2010; Tripathee et al. 2014b). During pre-monsoon period, a large scale of biomass burning occurs in Northern India and Nepal (Ram and Sarin 2010), and a large number of forest fires have been observed during the pre-monsoon in the IGP
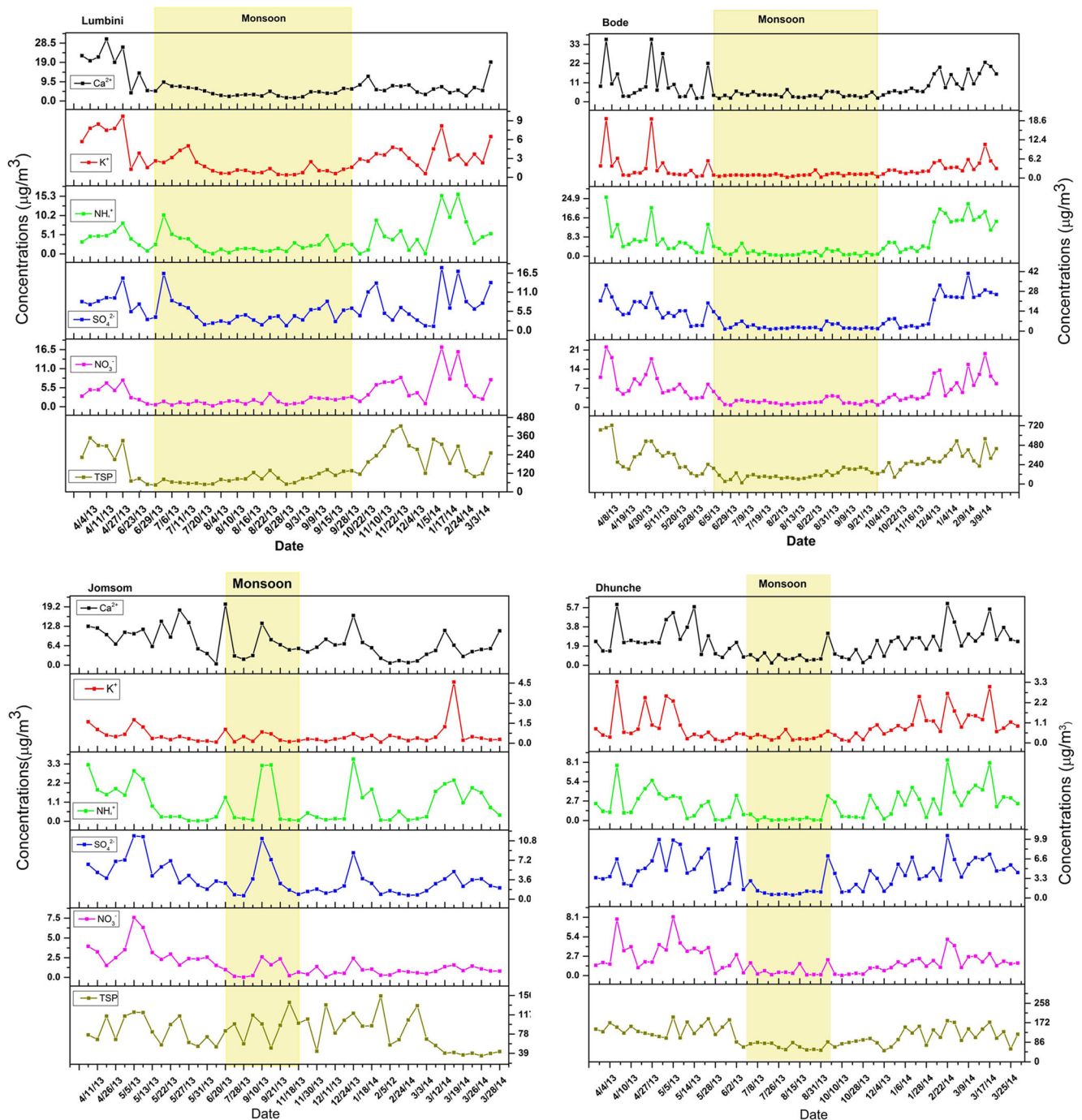
Fig. 4 Temporal variations of major soluble ions and TSP mass at four sites (April 2013 to May 2014)

(Vadrevu et al. 2012). At all four sites, K^+ concentrations were observed to be highest during pre-monsoon season suggesting the biomass burning and forest fire plays an important role during this period. However, K^+ could also originate from the interference of the crustal sources such as soil resuspension (Cheng et al. 2013; Wan et al. 2017), which should be taken into consideration in the urban and semi-urban sites. Therefore, we checked the correlation coefficient between Ca^{2+} and K^+ for all sites in Fig. S5. A significantly high

correlation coefficient was observed between Ca^{2+} and K^+ ($R^2 = 0.70$, $p < 0.01$) and ($R^2 = 0.81$, $p < 0.01$) for Lumbini and Bode, respectively, indicating that they originated from similar sources from soil resuspension at those urban and semi-urban sites. Meanwhile, poor correlation coefficient was observed between Ca^{2+} and K^+ ($R^2 = 0.05$, $p < 0.01$) and ($R^2 = 0.46$, $p < 0.01$) for Jomsom and Dhunche, suggesting K^+ must have mostly originated from biomass burning in the rural and remote sites.

Table 3 Seasonal concentrations of TSP mass and chemical species and contribution over the central Himalayas

Sites		TSP mass (µg/m³)	Cl⁻	NO₃⁻	SO₄²⁻	Na⁺	NH₄⁺	K⁺	Mg²⁺	Ca²⁺	Total Ions (µg/m³)	TWII/TSP%
Lumbini	Pre-monsoon	241.87	0.88	5.00	9.51	5.64	4.90	6.60	1.56	18.95	53.04	22.51
	SD	88.18	0.44	2.05	2.96	2.53	1.55	2.36	0.63	8.31	17.78	
	Monsoon	84.05	0.34	1.52	4.85	2.47	2.27	1.64	0.33	4.70	18.13	23.98
	SD	30.90	0.34	0.85	3.12	1.08	2.10	1.24	0.21	2.66	8.98	
	Post-monsoon	279.01	1.23	5.31	6.88	2.11	3.64	3.57	0.56	7.66	30.95	12.49
	SD	108.91	0.88	2.55	3.94	0.33	3.19	0.81	0.10	2.29	7.43	
	Winter	236.87	1.97	8.50	7.91	2.72	8.26	3.37	0.46	4.63	37.82	16.11
	SD	88.14	1.49	5.98	7.07	0.76	5.92	2.46	0.19	1.53	23.29	
	Annual average	161.14	0.79	3.66	6.40	3.03	3.77	3.05	0.60	7.67	28.96	21.01
	SD	105.95	0.89	3.58	4.25	1.82	3.55	2.45	0.55	6.75	18.72	
Jomsom	Pre-monsoon	64.98	0.33	2.39	4.77	2.35	1.28	0.77	0.35	8.76	21.01	37.08
	SD	30.37	0.43	1.75	2.76	0.87	0.98	0.95	0.14	4.14	8.37	
	Monsoon	73.50	0.18	1.18	4.13	2.99	0.71	0.46	0.34	7.18	17.17	31.30
	SD	28.95	0.10	1.00	3.52	1.83	1.10	0.37	0.29	6.74	12.30	
	Post-monsoon	98.35	0.12	0.66	1.48	2.08	0.21	0.22	0.24	5.19	10.21	13.13
	SD	40.99	0.06	0.50	0.41	1.03	0.19	0.09	0.04	0.67	1.19	
	Winter	104.63	0.25	0.75	2.32	2.99	0.73	0.38	0.23	5.29	12.95	12.81
	SD	30.61	0.29	0.63	2.30	1.41	1.12	0.19	0.19	4.72	9.76	
	Annual average	78.85	0.27	1.64	3.79	2.59	0.96	0.58	0.31	7.35	17.48	28.19
	SD	34.28	0.34	1.53	2.89	1.23	1.03	0.72	0.18	4.78	9.75	
Bode	Pre-monsoon	357.69	2.66	9.16	17.37	3.44	9.22	4.44	1.08	12.65	58.88	17.50
	SD	181.53	1.85	5.13	8.15	2.59	6.59	5.14	0.97	10.15	36.17	
	Monsoon	113.35	0.71	2.10	3.44	3.21	1.51	1.00	0.28	3.85	16.10	15.56
	SD	51.33	0.30	1.15	2.71	0.90	1.27	0.45	0.08	1.37	5.51	
	Post-monsoon	225.13	1.68	3.52	4.81	2.80	3.72	1.97	0.41	6.21	25.14	13.26
	SD	71.58	0.40	0.92	2.38	0.12	1.48	0.46	0.07	1.51	5.09	
	Winter	370.21	6.06	10.59	26.82	4.42	16.69	4.67	1.22	15.15	85.62	24.69
	SD	105.12	2.22	4.46	5.18	0.74	3.01	2.32	0.46	4.98	18.47	
	Annual average	238.24	2.17	5.38	10.96	3.36	6.13	2.62	0.65	8.19	39.22	17.75
	SD	162.24	2.25	4.72	10.08	1.65	6.57	3.39	0.68	7.46	32.98	
Dhunche	Pre-monsoon	137.56	0.47	2.84	5.16	2.02	2.83	1.28	0.25	2.92	17.78	13.66
	SD	31.89	0.81	1.81	2.31	1.76	2.00	1.49	0.13	1.51	8.56	
	Monsoon	69.97	0.15	0.79	2.27	1.27	0.86	0.37	0.08	1.02	6.81	9.41
	SD	13.88	0.11	0.89	2.79	0.44	1.22	0.17	0.07	0.76	5.61	
	Post-monsoon	89.27	0.15	0.49	2.22	2.88	1.20	0.45	0.10	1.07	8.56	9.60
	SD	8.72	0.06	0.49	1.47	1.00	1.21	0.36	0.07	0.78	4.51	
	Winter	114.46	0.36	1.92	4.52	4.35	2.75	1.07	0.24	2.33	17.53	16.10
	SD	43.74	0.28	1.22	2.67	0.77	2.48	0.62	0.07	0.95	7.47	
	Annual average	112.40	0.34	1.95	4.06	2.30	2.17	0.94	0.19	2.17	14.13	12.61
	SD	40.3	0.60	1.72	2.73	1.66	2.03	1.15	0.13	1.47	8.83	

In addition, to understand the atmospheric situation at different seasons during the sampling period, we checked the satellite derived information. The spatial distribution of fire spots observed from MODIS (MODerate-resolution Imaging Spectro-radiometer, both Terra and Aqua data set), which was obtained from Fire Information for Resource Management System (FIRMS, https://earthdata.nasa.gov/firms) at four different seasons during the sampling period is presented in Fig. 5. It is clearly observed from Fig. 5 that a large number of fire events are occurring in the pre-monsoon than at other seasons conforming that the majority of K⁺ at our study sites (mostly on rural sites) may have
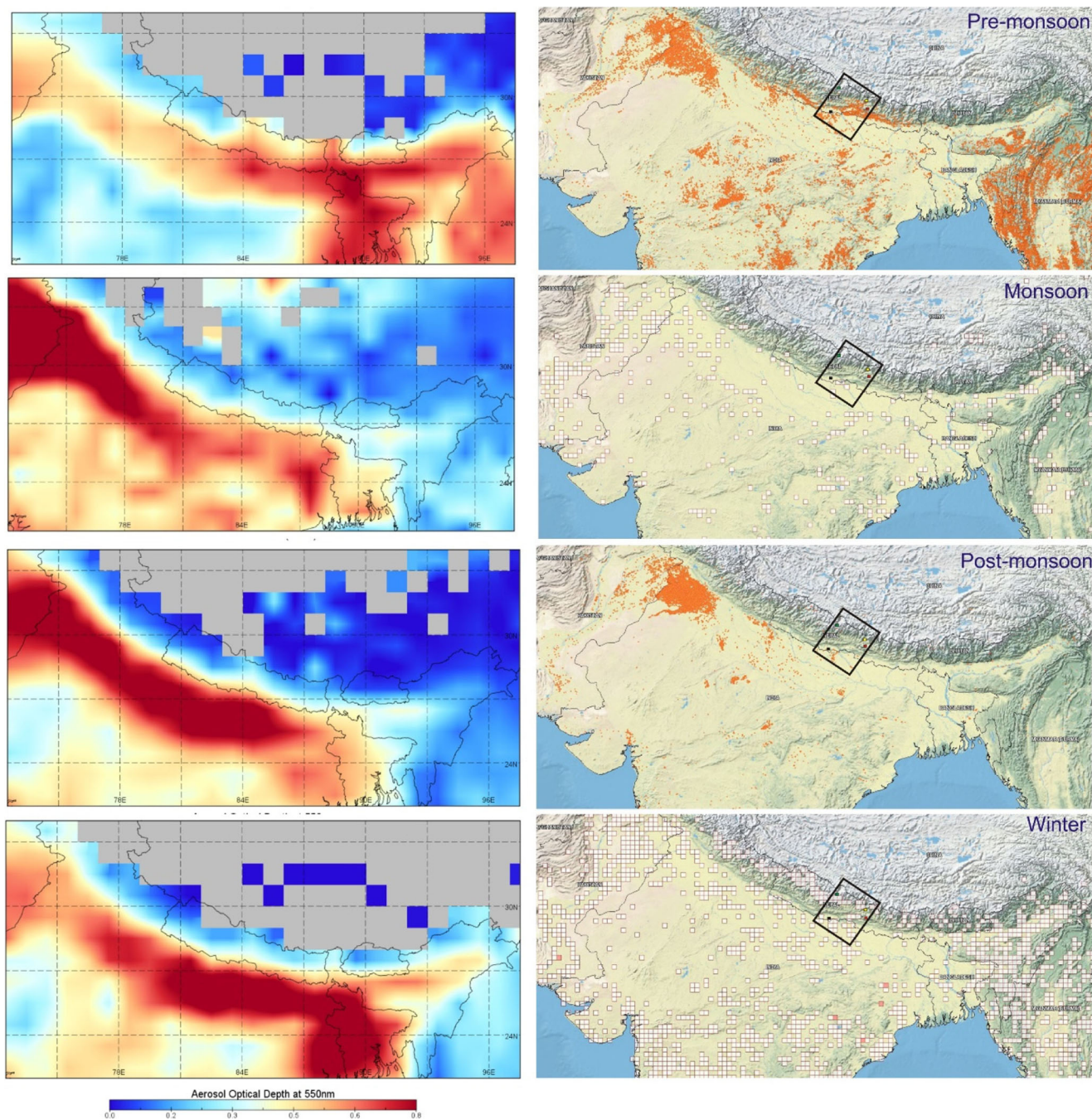
Fig. 5 Spatial distribution of AOD (left) and fire spots observed by MODIS (right) in different seasons (April 2013 to March 2014) (https://firms.modaps.eosdis.nasa.gov/firemap/)

been originated from biomass burning sources from the region. Furthermore, aerosol optical depth (AOD) over the sampling region at different seasons obtained from Terra satellite of MODIS is also presented in Fig. 5. The higher AOD values were observed during non-monsoon period at our sampling sites which further clarifies the heavier aerosol loadings during these periods. The pathways of air mass at different seasons and sources are explained in details in the next section below.

Possible sources of WSII and their transport pathways

Ratios of [NO$_3^-$]/[SO$_4^{2-}$] and sources of TSP

The ratios of [NO$_3^-$]/[SO$_4^{2-}$] at different seasons are shown in Table S2. Previous studies ascribed that the mass ratio of [NO$_3^-$]/[SO$_4^{2-}$] could be used as an indicator of the relative dominance of stationary (coal combustion, biomass burning) versus mobile sources (vehicular emissions)

of sulfur and nitrogen in the atmosphere (Xiao and Liu 2004; Yao et al. 2002). Higher $[NO_3^-]/[SO_4^{2-}]$ mass ratios (> 1) are attributed to the dominance of mobile pollutant sources and conversely lower ratios to that of stationary sources (Arimoto et al. 1996). The average annual mass ratios of $[NO_3^-]/[SO_4^{2-}]$ in this study were 0.68 ± 0.41, 0.44 ± 0.27, 0.63 ± 0.31, and 0.50 ± 0.39 at Lumbini, Jomsom, Bode, and Dhunche, respectively, which are lower than unity revealing that stationary emissions are the important and major contributors to atmospheric particles and vehicular emissions had minor contributions. At the semi-urban and remote sites (Jomsom and Dhunche), there is limited transportation facilities and vehicular emissions, for which the sources are mostly form stationary sources. In case of Bode and Lumbini, both the sites are surrounded by a large number of brick kilns and industries which may be responsible for their higher concentrations mass and lower $[NO_3^-]/[SO_4^{2-}]$ ratio. In details, in Lumbini, during post-monsoon and winter $[NO_3^-]/[SO_4^{2-}]$ ratio was 0.99 ± 0.75 and 0.98 ± 0.27, respectively, which is close to 1 attributing to mobile source (Table S2). Since, Lumbini is very close to the India and lies in the Indo-Gangetic Plains, the effects of long-range transport on local air pollutant could be significant during this period from mobile pollution sources. Moreover, in urban site Bode, during post-monsoon, their ratio was 0.85 ± 0.31, which may have been influenced by vehicular emissions from the city during the period. However, in other two remote sites, stationary sources are the major contributors of aerosol mass during all seasons over the year. The ratio was > 1 explaining the mobile source dominance as previously reported in the biggest city in the Tibetan Plateau, Lhasa (Wan et al. 2016); however, our sites had lower ratios inferring that stationary sources are of major sources of pollutants in the central Himalayas. In addition, secondary aerosols (e.g., NO_3^- and nss-SO_4^{2-}) are usually formed during the coal combustion process, biomass burning, and vehicular emissions (Seinfeld and Pandis 1998). The regression between these two ionic components is presented in Fig. 6. A strong correlation was observed for SO_4^{2-} and NO_3^- with R^2 values 0.72, 0.70, 0.74, and 0.54 for Lumbini, Jomsom, Bode, and Dhunche, respectively. Such a result confirms their commonality in behavior indicating that these ions originated from the common sources, i.e., anthropogenic such as fossil fuel burning, coal burning in the brick kilns emissions. Furthermore, NO_3^- and NH_4^+ in the urban and semi-urban sites had good relations ($R^2 \geq 0.66$, $p < 0.01$), suggesting their similar formation process in the urban atmosphere (Fig. S4). Meanwhile, in the rural sites, their poor relations ($R^2 \leq 0.36$, $p < 0.01$) suggest they must have released from distinct sources, as NH_4^+ could also be released from use of fertilizer and stationary wastes, and NO_3^- from fossil fuel combustion.

Marine contribution to aerosol composition

Non-sea-salt contribution of ionic components was evaluated assuming that the soluble Na^+ in aerosol was derived from the sea. Since the mass-based ratios of SO_4^{2-}/Na^+, K^+/Na^+, Mg^{2+}/Na^+, and Ca^{2+}/Na^+ in standard seawater are 0.252, 0.0370, 0.120, and 0.0385, respectively (Arakaki et al. 2014; Nair et al. 2005); the following equations were used to calculate non-sea salt (nss) value of SO_4^{2-}, K^+, Ca^{2+}, and Mg^{2+}, respectively:

$$nss-SO_4^{2-} = [SO_4^{2-}]-[Na^+] \times 0.2516 \qquad (6)$$

$$nss-K^+ = [K^+]-[Na^+] \times 0.0370 \qquad (7)$$

$$nss-Ca^{2+} = [Ca^{2+}]-[Na^+] \times 0.0385 \qquad (8)$$

$$nss-Mg^{2+} = [Mg^{2+}]--[Na^+] \times 0.12 \qquad (9)$$

The ratios of nss-SO_4^{2-}/SO_4^{2-}, nss-K^+/K^+, and nss-Ca^{2+}/Ca^{2+} in different seasons are depicted in Fig. 7. The higher ratio (> 0.92) of nss-Ca^{2+} was found at all sites during all seasons indicating marine contribution ($\leq$ 8%) to Ca^{2+} ion suggesting their continental contribution rather than marine origin. Prior studies in the central Himalayas are in agreement with our findings of higher dust loadings over the Himalayan atmosphere influenced by continental sources (Tripathee et al. 2014b, 2016b). While for nss-K^+/K^+, the ratio was (> 0.84) at two sites (Lumbini and Bode) during all seasons indicating marine contribution ($\leq$ 16%); however, in Jomsom, the ratio was (0.62–0.67) during monsoon, post-monsoon, and winter (33–38%) of marine contribution. Moreover, in Dhunche, nss-K^+ to K^+ ratio was 0.61 during post-monsoon suggesting that rural sites receive more sea salt K^+. In case for nss-SO_4^{2-} during pre-monsoon, nss-SO_4^{2-}/SO_4^{2-} ratio of (0.84–0.97) was observed at all the sites suggesting less impact on sea salt fraction of SO_4^{2-} during dry period. Meanwhile, the ratio in monsoon had a relatively lower ratio (0.66–0.77) at all sites, indicating that 23–34% of sea salt SO_4^{2-} could be transported to the central Himalayas by monsoon convection. At a glance, we can conclude that majority of soluble ions in aerosols in the central Himalayas was of continental origin and only few were of marine origin over the investigated year.

Principal component analysis

To investigate the possible sources, principal component analysis (PCA) was conducted. PCA analysis for water-soluble ions for four sampled sites were performed using SPSS 16.0 software and presented in Table 4. Principal components (PCs) were extracted with varimax rotation to provide the clearer pattern of variables loading in factors which makes data more explicable to interpret (Tripathee et al. 2016a; Xu et al. 2017). From the rotated component matrix for the PCA,

Fig. 6 Relationship between SO_4^{2-} and NO_3^- in four sampling sites
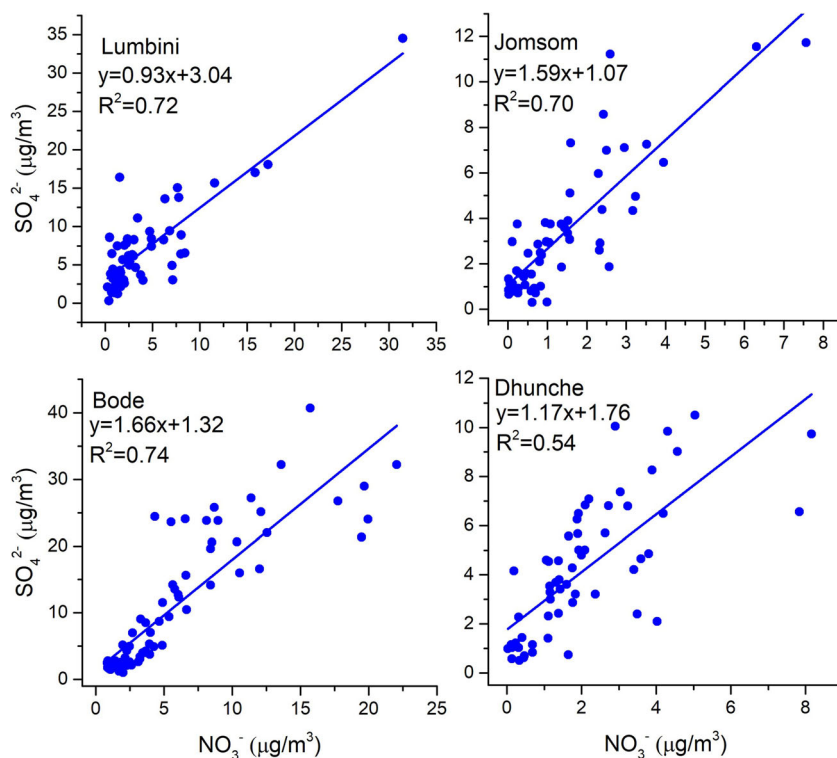

two PCs were extracted for three sites and three PCs were extracted for site Jomsom. The PCs loading were based on the eigenvalues > 1, which gives the robust results as its purpose is to normalize the number of PCs that can be extracted. In addition, the largest eigenvalues correspond to the PCs that are related with most of the co-variability among a number of observed data (Tripathee et al. 2016a).

In Lumbini, the first factor showed the high loadings of Ca^{2+}, Mg^{2+}, K^+, and Na^+ with a total variance of 60.47%. Such soluble ions are usually associated with crustal materials

from windblown dust, re-suspended dust particles including the dust from paved and unpaved roads (Nicolás et al. 2008) and Mg^{2+} has similar characteristics as Ca^{2+} (Wu et al. 2006). Moreover, K^+, which is considered as conventional tracer of biomass burning, existed in this factor suggesting that K^+ could have been mixed with interference of the crustal sources such as soil resuspension (Cheng et al. 2013), other than biomass burning or could have deposited at the same time in the atmosphere which has been explained in the earlier section. Second factor in Lumbini was associated with Cl^-, NO_3^-,

Fig. 7 Ratio of non-sea salt and their respective ionic fractions in different seasons over the central Himalayas
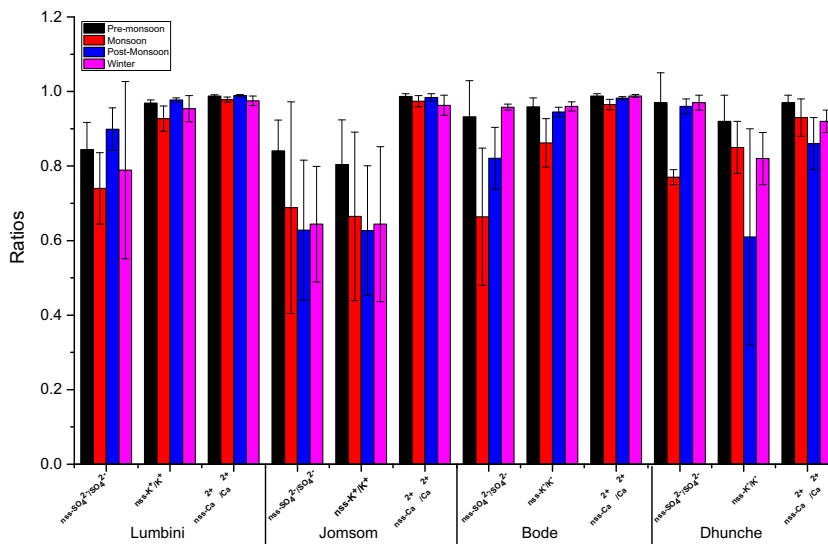
Table 4 Rotated principle component matrix for water-soluble ions in aerosols

WSIIs	Lumbini		Jomsom			Bode		Dhunche	
	PC1	PC2	PC 1	PC 2	PC 3	PC 1	PC 2	PC 1	PC 2
Cl^-	0.02	*0.88*	0.09	0.03	*0.91*	*0.89*	0.21	0.18	*0.88*
NO_3^-	0.18	*0.93*	*0.95*	0.10	0.09	*0.84*	0.43	*0.92*	0.02
SO_4^{2-}	0.43	*0.71*	*0.84*	0.36	0.18	*0.93*	0.26	*0.88*	0.07
Na^+	*0.91*	0.09	−0.14	*0.73*	0.51	0.09	*0.92*	0.02	*0.84*
NH_4^+	0.18	*0.91*	*0.58*	0.28	0.43	*0.85*	0.46	*0.81*	0.24
K^+	*0.83*	0.45	0.28	0.15	*0.90*	0.50	*0.81*	0.47	*0.82*
Mg^{2+}	*0.97*	0.19	0.41	*0.89*	0.06	0.58	*0.78*	*0.89*	0.30
Ca^{2+}	*0.98*	0.10	0.38	*0.85*	−0.002	0.55	*0.79*	*0.84*	0.40
Eigenvalue	4.83	2.05	4.13	1.52	1.13	4.01	3.22	4.01	2.45
% Variance	60.47	25.64	51.63	19.11	14.17	50.10	40.29	50.14	30.64
Cumulative %	60.47	86.11	51.63	70.75	84.92	50.10	90.39	50.14	80.78

Factor loadings considered as significant are marked in Italics

SO_4^{2-}, and NH_4^+ with a total variance of 25.64%. This result is obvious as these ions are derived from the anthropogenic activities in the atmosphere and these ions had a strong correlation coefficient (Fig. S5). The major sources for SO_4^{2-} and NO_3^- in the atmospheres are the oxidation of their gaseous precursors SO_2 and NO_x, which are emitted from various anthropogenic activities (Wang et al. 2006) and sources described in the earlier section. In the semiarid site Jomsom, the first factor with percentage variance of 51.63% was highly loaded with the anthropogenic soluble ions (NO_3^-, SO_4^{2-} and NH_4^+), suggesting that these ions were mainly derived from similar anthropogenic sources. Further, the second factor accounted for 19.11% of variance is loaded with Na^+, Mg^{2+}, and Ca^{2+} suggesting their concentrations are affected by soil particles or falling dust as explained earlier. Finally, factor 3 is dominated by Cl^- and K^+ and it accounted for 14.17% of the total variance, indicating that these two ions more likely originated from combustion process (Shen et al. 2009) such as biomass burning. In contrast, with Lumbini, K^+ in this region must have originated from biomass burning in the region, which is confirmed by the correlation coefficient between K^+ and Ca^{2+} (explained in the earlier section).

In urban site Bode, the first factor is dominated by Cl^-, NO_3^-, SO_4^{2-}, and NH_4^+ with percentage variance of 50.10% which is similar to the result from semi-urban site Lumbini. The second factor with 40.29% of variance was loaded by Na^+, K^+, Mg^{2+}, and Ca^{2+} suggesting that these soluble must have originated from natural crustal sources from construction activities (e.g., road, buildings, etc.) (Tripathee et al. 2014b) and mixed combustion sources. Likewise, in Lumbini, K^+ and Ca^{2+} in Bode had a very good relationship (Fig. S5), suggesting they might have originated form natural crustal source. In rural site Dhunche, with 50.14% of variance was loaded with mixed soluble ions such as anthropogenic (NO_3^-, SO_4^{2-}, and

NH_4^+) and crustal (Mg^{2+} and Ca^{2+}) suggesting that these ions may have deposited at the same time during sampling (Tripathee et al. 2014b). However, Cl^-, Na^+, and K^+ were loaded in the second factor with 30.64% of variance suggesting their similar sources, might have originated from mixed sources, i.e., sea salt and biomass burning. However, in the site like rural (Jomsom), the correlation coefficient between K^+ and Ca^{2+} was not very significant, suggesting majority of K^+ was originated from biomass burning rather than crustal sources.

Air mass back-trajectory analysis (potential source region and transport pathways)

The air mass backward trajectories are valuable to identify possible source regions and pathways, and to explore the influence of long-range transport of aerosols. Five-day backward air-mass trajectories for two rural remote sites were calculated using the HYSPLIT model (Draxler and Rolph 2003).The clusters of air mass back trajectories during each of the seasons are shown in Fig. 8. The air mass showed the distinctive seasonality, which were generally consistent with other descriptions of air circulation patterns in the previous studies (Bonasoni et al. 2010; Chen et al. 2017; Cong et al. 2015), corresponding to the South Asian monsoon regime. However, due to complex topography of the Himalayan region and the influence of local/regional transport processes related to thermal valley winds, back-trajectory results should be described with caution.

In pre-monsoon (March–May), about more than 80% air masses at all the sampling sites arrived from strong westerly pass through western Nepal, Northwest India, and Pakistan. During dry periods the climate in Himalayas is influenced by strong western disturbances (Bonasoni et al. 2010), which
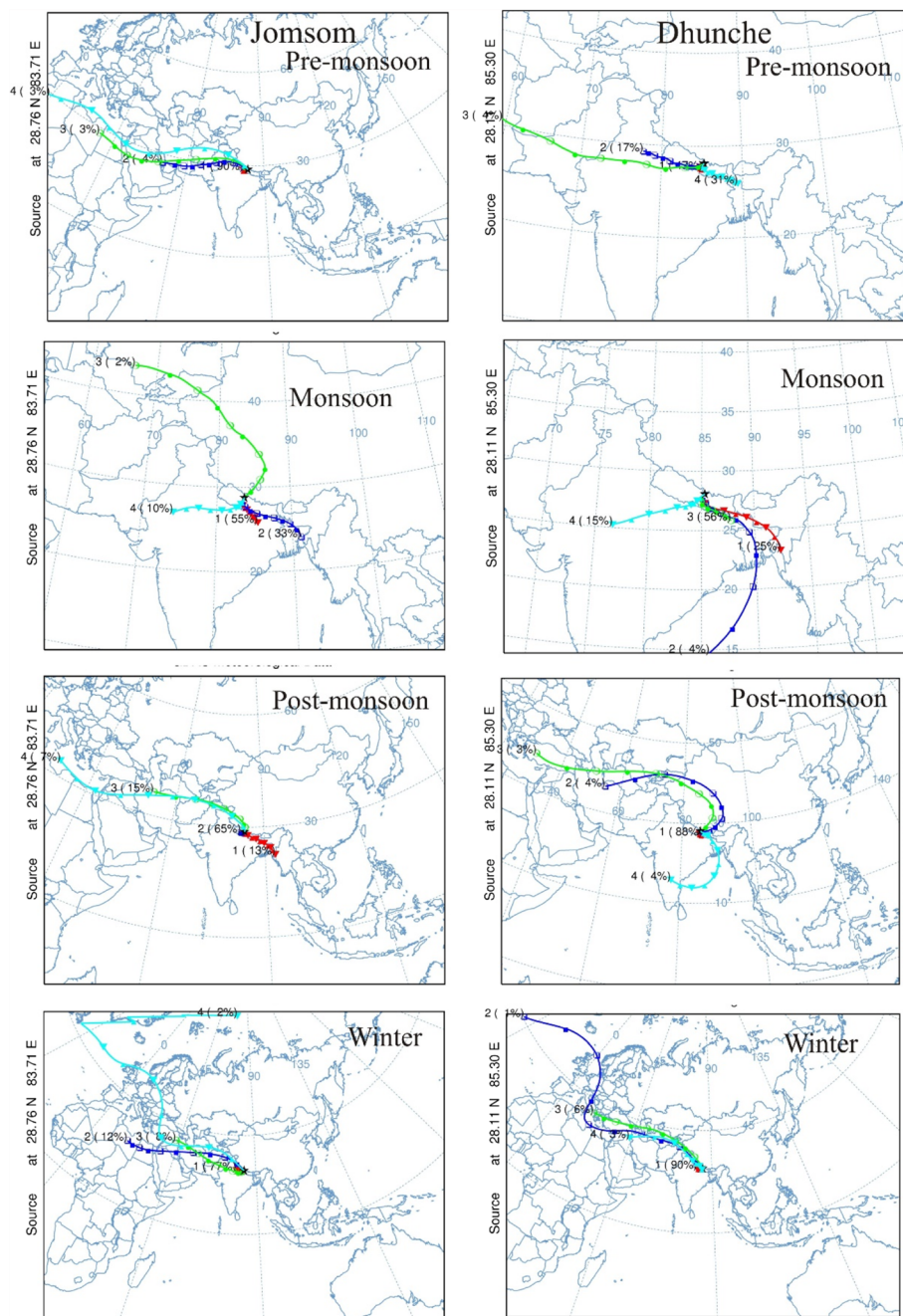
Fig. 8 Clusters of air mass back trajectories during each season in two remote sites of the central Himalayas

could transport significant amount of pollutants to our sampling locations from heavily polluted Indian cities. Furthermore, during the non-monsoon seasons (dry periods), the transport pathways of air masses arriving at our sampling sites were similar and northern India is the major source region. The results based on HYSPLIT back trajectories indicated potential aerosol source regions at our sampling sites. Meanwhile, the coarse resolution of the meteorological fields that drives HYSPLIT do not take into account thermally driven movements through Himalayan valleys and up slopes (Chen et al. 2017). Therefore, the local orographic effect on

air pollutant transport may also paly significant role which should be taken into consideration. In monsoon (June–September), most of the air masses arrived our sites from Bangladesh and northeast India, which bring moisture originating from Bay of Bengal with polluted aerosols from the urban cities from those regions. In post-monsoon (October–November), majority of the air masses 65% were local arrived from North India to our sites. In winter (December–February), there was similar transport pathways as during the pre-monsoon period (dry period), suggesting that the transboundary aerosol transport to the central Himalayas

might be significant during these periods. These scenarios could also be supported by higher number of fire spots observed over the region and furthermore, higher AOD during the dry periods as reveled by Fig. 5.

Summary and conclusions

Long-term continuous observations of aerosol soluble chemical composition (from April 2013 to March 2014) were conducted and analyzed for the major WSIIs at four sites representing different geographic locations over the southern side of the central Himalayas. The spatial variation of annual average TSP mass concentration and total soluble ions followed the order Bode (urban)>Lumbini (semi-urban IGP site)>Dhunche (rural)>Jomsom (semiarid rural) indicating higher aerosol and soluble ions loadings over urban and IGP sites. The major compound of TSP was $(NH_4)_2SO_4$ at three sites and NH_4HSO_4 in semiarid site in the central Himalayas. The anthropogenic aerosols (e.g., SO_4^{2-}, NO_3^-, and NH_4^+) were highest in urban site Bode followed by IGP site Lumbini. However, crustal ion Ca^{2+} had a similar magnitude over urban, IGP, and semiarid sites as the semiarid site receives low precipitation. Interestingly, the concentrations of Na^+ were higher than the Cl^- at all our sites suggesting that there must have been loss process of Cl^- on sea salt particles. Three sites showed the clear and striking seasonality with highest concentrations during pre-monsoon and winter (dry periods) and lower concentrations during monsoon as increase in precipitation washes out aerosols during monsoon. However, no clear seasonal variation was observed in semiarid site Jomsom which must be attributed to little precipitation. Furthermore, back-trajectories analyses at different seasons suggested that the air mass transported through Northwest India, Pakistan, and Indo-Gangetic Plains during the dry periods (pre-monsoon and winter), which may have resulted in higher loadings of soluble ion during those period over the central Himalayas. Nevertheless, seasonal differences in atmospheric and meteorological conditions may also effect the variation of soluble ions in the aerosols. The $[NO_3^-/SO_4^{2-}]$ ratio suggested that sources of aerosols are mostly from stationary source at all sampled sites, meanwhile mobile sources were dominant during post-monsoon and winter in IGP site Lumbini. The PCA results showed three distinct sources of ions: (1) secondary anthropogenic aerosols from stationary sources such as brick kilns emission, coal combustion and mobile vehicular emissions; (2) natural mineral aerosol and re-suspended fugitive road dust; (3) mixed sea salt and biomass burning over the central Himalayas. However, this study also suggests that K^+ is derived from crustal dusts in semi-urban and urban sites and from biomass burning and sea salt contribution on the rural sites in the central Himalayas.

Moreover, further long-term comprehensive works on carbonaceous particles and biomass burning tracers are needed to better understand the sources and transport of aerosols particles from combustion activities in the region. This study provides the insights into spatial distribution (urban, semi-urban IGP region, rural, and semiarid region) and seasonal variations of soluble ions over the central Himalayas which is helpful for creating valuable dataset for future studies. In addition, atmospheric environment situation has been well documented which can also be useful for policy maker to formulate new policies on air quality in the region.

References

Ali K, Budhavant KB, Safai PD, Rao PS (2012) Seasonal factors influencing in chemical composition of total suspended particles at Pune, India. Sci Total Environ 414:257–267

Al-Khashman OA (2005) Ionic composition of wet precipitation in the Petra Region, Jordan. Atmos Res 78:1–12

Anderson RR, Martello DV, Rohar PC, Strazisar BR, Tamilia JP, Waldner K, White CM, Modey WK, Mangelson NF, Eatough DJ (2002) Sources and composition of PM2. 5 at the National Energy Technology Laboratory in Pittsburgh during July and August 2000. Energy Fuel 16:261–269

Arakaki T et al (2014) Spatial and temporal variations of chemicals in the TSP aerosols simultaneously collected at three islands in Okinawa, Japan. Atmos Environ 97:479–485

Arimoto R, Duce R, Savoie D, Prospero J, Talbot R, Cullen J, Tomza U, Lewis N, Ray B (1996) Relationships among aerosol constituents from Asia and the North Pacific during PEM-West A. J Geophys Res Atmos 101:2011–2023

Bonasoni P et al (2010) Atmospheric brown clouds in the Himalayas: first two years of continuous observations at the Nepal Climate Observatory-Pyramid (5079 m). Atmos Chem Phys 10:7515–7531

Cao J-J, Xu B-Q, He J-Q, Liu X-Q, Han Y-M, Wang G-h, Zhu C-s (2009) Concentrations, seasonal variations, and transport of carbonaceous aerosols at a remote mountainous region in western China. Atmos Environ 43:4444–4452

Carrico CM, Bergin MH, Shrestha AB, Dibb JE, Gomes L, Harris JM (2003) The importance of carbon and mineral dust to seasonal aerosol properties in the Nepal Himalaya. Atmos Environ 37:2811–2824

Chelani AB, Gajghate DG, Chalapatirao CV, Devotta S (2010) Particle size distribution in ambient air of Delhi and its statistical analysis. Bull Environ Contam Toxicol 85:22–27

Cheng Y, Engling G, He K-B, Duan F-K, Ma Y-L, Du Z-Y, Liu J-M, Zheng M, Weber RJ (2013) Biomass burning contribution to Beijing aerosol. Atmos Chem Phys 13:7765–7781

Chen P, Li C, Kang S, Rupakheti M, Panday AK, Yan F, Li Q, Zhang Q, Guo J, Ji Z, Rupakheti D et al (2017) Characteristics of particulate-phase polycyclic aromatic hydrocarbons (PAHs) in the atmosphere over the central Himalayas. Aerosol Air Qual Res. https://doi.org/10.4209/aaqr.2016.09.0385

Cong Z, Kang S, Liu X, Wang G (2007) Elemental composition of aerosol in the Nam Co region, Tibetan Plateau, during summer monsoon season. Atmos Environ 41:1180–1187

Cong Z, Kang S, Kawamura K, Liu B, Wan X, Wang Z, Gao S, Fu P (2015) Carbonaceous aerosols on the south edge of the Tibetan Plateau: concentrations, seasonality and sources. Atmos Chem Phys 15:1573–1584

Davidson CI, Phalen RF, Solomon PA (2005) Airborne particulate matter and human health: a review. Aerosol Sci Technol 39:737–749

Decesari S, Facchini MC, Carbone C, Giulianelli L, Rinaldi M, Finessi E, Fuzzi S, Marinoni A, Cristofanelli P, Duchi R, Bonasoni P, Vuillermoz E, Cozic J, Jaffrezo JL, Laj P (2010) Chemical composition of PM10 and PM1 at the high-altitude Himalayan station Nepal Climate Observatory-Pyramid (NCO-P) (5079 m a.s.l.) Atmos Chem Phys 10:4583–4596

Deshmukh DK, Deb MK, Tsai YI, Mkoma SL (2011) Water soluble ions in PM2. 5 and PM1 aerosols in Durg city, Chhattisgarh, India. Aerosol Air Qual Res 11:696–708

Deshmukh DK, Tsai YI, Deb MK, Zarmpas P (2012) Characteristics and sources of water-soluble ionic species associated with PM10 particles in the ambient air of central India. Bull Environ Contam Toxicol 89:1091–1097

Draxler RR, Rolph G (2003) HYSPLIT (HYbrid single-particle Lagrangian integrated trajectory) model access via NOAA ARL READY website (http://www.arl.noaa.gov/ready/hysplit4.html). NOAA Air Resources Laboratory, Silver Spring

Gao X, Xue L, Wang X, Wang T, Yuan C, Gao R, Zhou Y, Nie W, Zhang Q, Wang W (2012) Aerosol ionic components at Mt. Heng in central southern China: abundances, size distribution, and impacts of long-range transport. Sci Total Environ 433:498–506

Kang S, Xu Y, You Q, Flügel W-A, Pepin N, Yao T (2010) Review of climate and cryospheric change in the Tibetan Plateau. Environ Res Lett 5:015101

Kumar A, Sarin MM (2010) Atmospheric water-soluble constituents in fine and coarse mode aerosols from high-altitude site in western India: long-range transport and seasonal variability. Atmos Environ 44:1245–1254

Kumar P, Yadav S (2016) Seasonal variations in water soluble inorganic ions, OC and EC in PM10 and PM>10 aerosols over Delhi: influence of sources and meteorological factors. Aerosol Air Qual Res 16:1165–1178

Lelieveld J, Crutzen P, Ramanathan V, Andreae M, Brenninkmeijer C, Campos T, Cass G, Dickerson R, Fischer H, De Gouw J (2001) The Indian Ocean experiment: widespread air pollution from South and Southeast Asia. Science 291:1031–1036

Ming J, Zhang D, Kang S, Tian W (2007) Aerosol and fresh snow chemistry in the East Rongbuk Glacier on the northern slope of Mt. Qomolangma (Everest). J Geophys Res Atmos 112(D15). https://doi.org/10.1029/2007JD008618

Mouli PC, Mohan SV, Reddy SJ (2006) Chemical composition of atmospheric aerosol (PM 10) at a semi-arid urban site: influence of terrestrial sources. Environ Monit Assess 117:291–305

Nair PR, Parameswaran K, Abraham A, Jacob S (2005) Wind-dependence of sea-salt and non-sea-salt aerosols over the oceanic environment. J Atmos Sol Terr Phys 67:884–898

Nicolás JF, Galindo N, Yubero E, Pastor C, Esclapez R, Crespo J (2008) Aerosol inorganic ions in a semiarid region on the Southeastern Spanish Mediterranean Coast. Water Air Soil Pollut 201:149–159

Pandey P, Khan AH, Verma AK, Singh KA, Mathur N, Kisku GC, Barman SC (2012) Seasonal trends of PM2.5 and PM10 in ambient air and their correlation in ambient air of Lucknow city, India. Bull Environ Contam Toxicol 88:265–270

Pathak RK, Wu WS, Wang T (2009) Summertime PM 2.5 ionic species in four major cities of China: nitrate formation in an ammonia-deficient atmosphere. Atmos Chem Phys 9:1711–1722

Ram K, Sarin MM (2010) Spatio-temporal variability in atmospheric abundances of EC, OC and WSOC over northern India. J Aerosol Sci 41:88–98

Ram K, Sarin MM, Hegde P (2010) Long-term record of aerosol optical properties and chemical composition from a high-altitude site (Manora Peak) in Central Himalaya. Atmos Chem Phys 10:11791–11803

Ram K, Sarin M, Sudheer A, Rengarajan R (2012) Carbonaceous and secondary inorganic aerosols during wintertime fog and haze over urban sites in the Indo-Gangetic Plain. Aerosol Air Qual Res 12:359–370

Ramanathan V, Ramana MV (2005) Persistent, widespread, and strongly absorbing haze over the Himalayan foothills and the Indo-Gangetic Plains. Pure Appl Geophys 162:1609–1626

Ramanathan V, Chung C, Kim D, Bettge T, Buja L, Kiehl JT, Washington WM, Fu Q, Sikka DR, Wild M (2005) Atmospheric brown clouds: impacts on South Asian climate and hydrological cycle. Proc Natl Acad Sci U S A 102:5326–5333

Rastogi N, Sarin MM (2005) Long-term characterization of ionic species in aerosols from urban and high-altitude sites in western India: role of mineral dust and anthropogenic sources. Atmos Environ 39:5541–5554

Safai PD, Budhavant KB, Rao PSP, Ali K, Sinha A (2010) Source characterization for aerosol constituents and changing roles of calcium and ammonium aerosols in the neutralization of aerosol acidity at a semi-urban site in SW India. Atmos Res 98:78–88

Satsangi A, Pachauri T, Singla V, Lakhani A, Kumari KM (2013) Water soluble ionic species in atmospheric aerosols: concentrations and sources at Agra in the Indo-Gangetic Plain (IGP). Aerosol Air Qual Res 13:1877–1889

Seinfeld JH, Pandis SN (1998) Atmospheric chemistry and physics: from air pollution to climate change. John Wiley, New York

Shen Z, Cao J, Arimoto R, Han Z, Zhang R, Han Y, Liu S, Okuda T, Nakao S, Tanaka S (2009) Ionic composition of TSP and PM 2.5 during dust storms and air pollution episodes at Xi'an, China. Atmos Environ 43:2911–2918

Shrestha AB, Wake CP, Dibb JE (1997) Chemical composition of aerosol and snow in the high Himalaya during the summer monsoon season. Atmos Environ 31:2815–2826

Shrestha AB, Wake CP, Dibb JE, Whitlow SI (2002) Aerosol and precipitation chemistry at a remote Himalayan site in Nepal. Aerosol Sci Technol 36:441–456

Sigdel M, Ma Y (2016) Evaluation of future precipitation scenario using statistical downscaling model over humid, subhumid, and arid region of Nepal—a case study. Theor Appl Climatol 123:453–460

Sun J, Qin D, Mayewski PA, Dibb JE, Whitlow S, Li Z, Yang Q (1998) Soluble species in aerosol and snow and their relationship at Glacier 1, Tien Shan, China. J Geophys Res Atmos 103:28021–28028

Sun Y, Zhuang G, Tang A, Wang Y, An Z (2006) Chemical characteristics of PM2. 5 and PM10 in haze—fog episodes in Beijing. Environ Sci Technol 40:3148–3155

Tripathee L, Kang S, Huang J, Sharma CM, Sillanpää M, Guo J, Paudyal R (2014a) Concentrations of trace elements in wet deposition over the central Himalayas, Nepal. Atmos Environ 95:231–238

Tripathee L, Kang S, Huang J, Sillanpää M, Sharma C, Lüthi Z, Guo J, Paudyal R (2014b) Ionic composition of wet precipitation over the southern slope of central Himalayas, Nepal. Environ Sci Pollut Res 21:2677–2687

Tripathee L, Kang S, Rupakheti D, Zhang Q, Bajracharya RM, Sharma CM, Huang J, Gyawali A, Paudyal R, Sillanpää M (2016a) Spatial distribution, sources and risk assessment of potentially toxic trace elements and rare earth elements in soils of the Langtang Himalaya, Nepal. Environ Earth Sci 75(19):1332

Tripathee L, Kang S, Rupakheti D, Zhang Q, Huang J, Sillanpää M (2016b) Water-soluble ionic composition of aerosols at urban location in the foothills of Himalaya, Pokhara Valley, Nepal. Atmosphere 7:102

Vadrevu KP, Ellicott E, Giglio L, Badarinath K, Vermote E, Justice C, Lau WK (2012) Vegetation fires in the himalayan region—aerosol load, black carbon emissions and smoke plume heights. Atmos Environ 47:241–251

Wan X, Kang S, Xin J, Liu B, Wen T, Wang P, Wang Y, Cong Z (2016) Chemical composition of size-segregated aerosols in Lhasa city, Tibetan Plateau. Atmos Res 174-175:142–150

Wan X, Kang S, Li Q, Rupakheti D, Zhang Q, Guo J, Chen P, Tripathee L, Rupakheti M, Panday AK (2017) Organic molecular tracers in the atmospheric aerosols from Lumbini, Nepal, in the northern Indo-Gangetic Plain: influence of biomass burning. Atmos Chem Phys 17:8867–8885

Wang Y, Zhuang G, Tang A, Yuan H, Sun Y, Chen S, Zheng A (2005) The ion chemistry and the source of PM2.5 aerosol in Beijing. Atmos Environ 39:3771–3784

Wang Y, Zhuang G, Zhang X, Huang K, Xu C, Tang A, Chen J, An Z (2006) The ion chemistry, seasonal cycle, and sources of PM2.5 and TSP aerosol in Shanghai. Atmos Environ 40:2935–2952

Wu D, Tie X, Deng X (2006) Chemical characterizations of soluble aerosols in southern China. Chemosphere 64:749–757

Xiao H-Y, Liu C-Q (2004) Chemical characteristics of water-soluble components in TSP over Guiyang, SW China, 2003. Atmos Environ 38:6297–6306

Xu J, Wang Z, Yu G, Qin X, Ren J, Qin D (2014) Characteristics of water soluble ionic species in fine particles from a high altitude site on the northern boundary of Tibetan Plateau: mixture of mineral dust and anthropogenic aerosol. Atmos Res 143:43–56

Xu J-S, Xu M-X, Snape C, He J, Behera SN, Xu H-H, Ji D-S, Wang C-J, Yu H, Xiao H, Jiang Y-J, Qi B, Du R-G (2017) Temporal and spatial variation in major ion chemistry and source identification of secondary inorganic aerosols in northern Zhejiang Province, China. Chemosphere 179:316–330

Yang Y, Zhou R, Yan Y, Yu Y, Liu J, Du Z, Wu D (2016) Seasonal variations and size distributions of water-soluble ions of atmospheric particulate matter at Shigatse, Tibetan Plateau. Chemosphere 145:560–567

Yao X, Chan CK, Fang M, Cadle S, Chan T, Mulawa P, He K, Ye B (2002) The water-soluble ionic composition of PM2.5 in Shanghai and Beijing, China. Atmos Environ 36:4223–4234

Zhang N, He Y, Theakstone WH, Pang H (2010) Chemical composition of aerosol and fresh snow and tourism influences at Baishui Glacier No. 1 from Mt. Yulong, southeastern Tibetan Plateau. J Earth Sci 21:199–209

Zhang N, He Y, Wang C, He X, Xin H (2011) The chemical characteristic of soluble ions in total suspended particles (TSP) at Lijiang winter time. Environ Sci 32:26–33

Zhang N, Cao J, Ho K, He Y (2012) Chemical characterization of aerosol collected at Mt. Yulong in wintertime on the southeastern Tibetan Plateau. Atmos Res 107:76–85

Zhao Z, Cao J, Shen Z, Xu B, Zhu C, Chen LWA, Su X, Liu S, Han Y, Wang G, Ho K (2013) Aerosol particles at a high-altitude site on the southeast Tibetan Plateau, China: implications for pollution transport from South Asia. J Geophys Res Atmos 118:11,360–11,375